HHS Public Access

Author manuscript

Biochemistry. Author manuscript; available in PMC 2018 April 04.

Published in final edited form as:

Biochemistry. 2017 April 04; 56(13): 1899–1910. doi:10.1021/acs.biochem.7b00060.

Biochemical characterization of AP lyase and m^{6}A demethylase activities of human AlkB homolog 1 (ALKBH1)

Tina A. Müller[†], **Michael A. Tobar**[†], **Madison N. Perian**[‡], and **Robert P. Hausinger**[†,§,*]

[†]Department of Microbiology and Molecular Genetics, Michigan State University, East Lansing, Michigan 48824

[‡]Biology Department, Kalamazoo College, Kalamazoo, Michigan 49006

[§]Department of Biochemistry and Molecular Biology, Michigan State University, East Lansing, Michigan 48824

Abstract

Alkbh1 is one of nine mammalian homologs of *Escherichia coli* AlkB, a 2-oxoglutarate-dependent dioxygenase that catalyzes direct DNA repair by removing alkyl lesions from DNA. Six distinct enzymatic activities have been reported for Alkbh1, including hydroxylation of variously methylated DNA, mRNA, tRNA, or histone substrates along with the cleavage of DNA at apurinic/apyrimidinic (AP) sites followed by covalent attachment to the 5′-product. The studies described here extend the biochemical characterization for two of these enzymatic activities using human ALKBH1: the AP lyase and 6-methyl adenine DNA demethylase activities. The steady-state and single-turnover kinetic parameters for ALKBH1 cleavage of AP sites in DNA were determined and shown to be comparable to other AP lyases. The α,β-unsaturated aldehyde of the 5′-product arising from DNA cleavage reacts predominantly with C129 of ALKBH1, but secondary sites also generate covalent adducts. The 6-methyl adenine demethylase activity was examined with a newly developed assay using a methylation-sensitive restriction endonuclease, and the enzymatic rate was found to be very low. Indeed, the demethylase activity was less than half that of the AP lyase activity when ALKBH1 samples were assayed using identical buffer conditions. The two enzymatic activities were examined using a series of site-directed variant proteins, revealing the presence of distinct, but partially overlapping active sites for the two reactions. We postulate that the very low 6-methyl adenine oxygenase activity associated with ALKBH1 is unlikely to represent the major function of the enzyme in this cell, while the cellular role of the lyase activity (including its subsequent covalent attachment to DNA) remains uncertain.

TOC image

[*]**Corresponding Author:** Telephone: 517-884-5404. hausinge@msu.edu.

Supporting Information

The supporting information is available free of charge on the ACS Publications website at DOI: xxx/acs.biochem.xxx
A supplementary figure is provided.

Notes

The authors declare no competing financial interest.

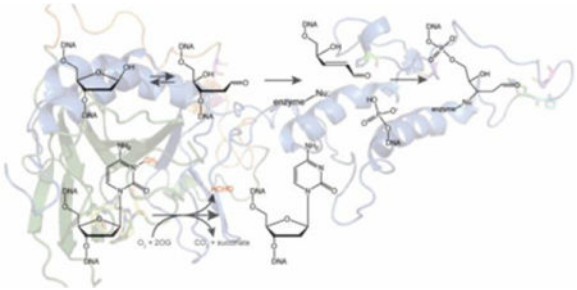

The nitrogenous bases of DNA and RNA undergo methylation and other types of modification that result in nucleic acid damage or that act as epigenetic signals during the development and function of a cell. The cytotoxic and mutagenic lesions are removed by enzymes that function in specific repair pathways, and epigenetic modifications are also known to be acted on by proteins that allow the signals to be reversible and dynamic.[1–6] A particularly well-characterized enzyme involved in nucleic acid demethylation is AlkB of *Escherichia coli* which catalyzes the removal of alkyl groups from DNA bases.[7, 8] AlkB belongs to the diverse group of Fe(II)/2-oxoglutarate (2OG)-dependent dioxygenases.[9–11] The enzyme catalyzes the oxidative decarboxylation of the co-substrate 2OG while concomitantly hydroxylating *N*-alkyl groups on DNA bases such as 1-methyl adenine (m^1A) or 3-methyl cytosine (m^3C). The hydroxylated intermediate is unstable and decomposes with release of the methyl group as formaldehyde while restoring the native base.

Mammals have nine AlkB homologs called Alkbh1 through 8 and FTO for fat mass and obesity associated protein.[12–14] These AlkB homologs play diverse cellular roles and catalyze both direct DNA repair and the reversal of epigenetic modifications. Alkbh2 and Alkbh3 possess the same demethylase activity as AlkB, with the former enzyme being the most important protein for repair of alkylated DNA bases in mammals.[15–17] Alkbh3 hydroxylates methyl lesions in single-stranded (ss) DNA as well as m^1A in mRNA, thereby expanding the substrate range to RNA.[18] Alkbh5 and FTO also act on RNA,[19–22] but these enzymes demethylate 6-methyl adenine (m^6A) in this substrate *in vitro*, affecting mRNA stability.[1] *In vivo*, Alkbh5 plays a role in fertility while FTO is important for controlling body weight in mice and humans.[23, 24] Alkbh8 is an unusual member of the family and contains RNA-recognition and methyltransferase domains in addition to the AlkB domain. This enzyme hydroxylates 5-methylated uridines in the wobble position of tRNA, thereby playing a role in translation.[3, 10, 25] In 2013, the substrate range of AlkB homologs was expanded beyond nucleic acids to proteins, when Alkbh4 was implicated in actin demethylation and found to be important for cell division.[26] While the substrate of Alkbh7 is unknown, this AlkB homolog was identified as a mitochondrial protein associated with two different cellular functions. One study showed that the enzyme is involved in programmed necrosis, whereas another group showed that Alkbh7-deficient mice are obese and suggested that the protein plays a role in fatty acid chain oxidation.[27, 28] Last, neither a functional role nor a substrate has been associated with Alkbh6.

Alkbh1 (or ALKBH1- when specifically referring to the human enzyme) is the mammalian homolog most closely related to bacterial AlkB.[12] Despite this similarity in sequence, its

cellular role and enzymatic activity have been matters of dispute. Studies with *Alkbh1*$^{-/-}$ mice initially indicated that this homolog is important for *in utero* development and later revealed that Alkbh1-deficient animals are born at a lower than expected Mendelian ratio, are smaller than their wild-type littermates, and, most intriguingly, show a distorted gender bias with more males than females born.[29–31] Six distinct enzymatic activities have been reported for Alkbh1 (Scheme 1). In 2008, Krokan and colleagues showed that the human protein has weak demethylase activity on m^3C in ssDNA and RNA.[32] In 2012, Alkbh1 was implicated in demethylation of a methyl-lysyl residue of histone H2A in mouse stem cells.[33] Wu *et al.* (2016) identified m^6A of DNA as a substrate for the mouse embryonic stem (ES) cell enzyme, showed that the absence of this modification led to epigenetic gene silencing, and suggested that it probably plays a role in human gene expression and X chromosome inactivation.[34] In contrast to this nuclear function, Bohnsack and colleagues (2016) described a role for ALKBH1 as a mitochondrial tRNA hydroxylase, which oxidizes 5-methyl cytosine at position 34 (m^5C34) to 5-formyl cytosine in $tRNA^{Met}$ and is therefore involved in mitochondrial translation.[35] Liu *et al.* (2016) similarly showed ALKBH1 acts on tRNA, but they found that it demethylates m^1A at position 58 (m^1A58) in cytoplasmic tRNA and that it therefore plays a role in translation.[36] Finally, we discovered a non-oxidative role for ALKBH1; it catalyzes the cleavage of DNA at abasic (apyrimidinic/apurinic or AP) sites.[37, 38] AP lyase activity also has been reported for the enzyme from *Schizosaccharomyces pombe*.[39]

Here, we extend the biochemical characterization for two of the six described enzymatic activities of ALKBH1; i.e., its AP lyase and m^6A DNA demethylase activity. We determine kinetic parameters for the AP lyase activity and provide more insights into the formation of the covalent bond between ALKBH1 and the α,β-unsaturated aldehyde of the 5′-product following DNA cleavage. In order to examine the m^6A demethylase activity, we develope a new assay and examine the turnover rate. We also determine and compare the turnover rates for both enzymatic activities for the WT and variant proteins and postulate two distinct, but partially overlapping, active sites for the two catalytic mechanisms.

RESULTS

Kinetic characterization of the AP lyase activity of ALKBH1

We carried out a series of activity assays to examine the kinetic behavior of ALKBH1 by monitoring the release of the 3′-DNA product under steady-state assay conditions. We incubated different concentrations of ALKBH1 with excess 3′-fluorescein (FAM)-labeled oligo_AP1 (Table 1) while monitoring product formation over time (Fig. 1A). Product formation was biphasic, with a fast initial phase followed by a linear steady-state phase. We plotted the intercepts of these lines against the protein concentrations used in the assays (Fig. 1B). The slope calculated from these lines represents the fraction of active protein in the sample, a value needed to determine the intrinsic turnover rate. Protein concentrations measured using standard assays often overestimate the enzyme concentration due to the presence of inactive protein or impurities.[40–43] Indeed, our analysis revealed that only about 22.0±1.4% of the ALKBH1 protein is active as purified from recombinant *E. coli* cells expressing the human gene. This finding corroborates previous results when we found that

ALKBH1 formed substoichiometric amounts of products and speculated that the protein might be partially inactive.[38] In order to calculate the valid steady-state turnover rate, we replotted the slopes of the curves shown in Fig. 1A against the calculated active protein concentration in each assay and the resulting slope was determined. This analysis revealed that ALKBH1 turns over 0.028±0.003 AP sites min^{-1} (Fig. 1C).

The biphasic behavior noted above (Fig. 1A) is a typical feature of DNA repair enzymes and indicates that a step after chemical catalysis is rate limiting in the overall reaction. In order to separate the steady-state turnover rate from the chemical catalysis rate of ALKBH1, we examined DNA cleavage under single-turnover conditions, with the enzyme concentration in excess over the substrate concentration (Fig. 1D). The pre-steady state rate was calculated as previously described,[43] providing a k_{obs} of 0.069±0.005 min^{-1}. We also determined the k_{obs} values with double-stranded (ds) DNA. Two dsDNA substrates were used; one with one AP site (oligo_AP1 annealed to oligo_AP2, Table 1) and one with two AP sites on opposing strands in close proximity to each other (oligo_AP1 annealed to oligo_AP3, Table 1). The single-turnover rates with dsDNA were 0.020±0.002 min^{-1} for the dsDNA with one AP site and 0.028±0.002 min^{-1} for the substrate with two AP sites (Fig. 1 D).

Mechanism of formation of the ALKBH1-DNA adduct and 5′-product release

Subsequent to catalysis of the AP lyase reaction by ALKBH1, the enzyme forms a covalent bond to its 5′-DNA product, thus making it a single-turnover enzyme.[37] We had previously hypothesized that adduct formation may occur either by a nucleophilic attack on C3′ of the α,β-unsaturated aldehyde at the 3′-end of the 5′-DNA product or by a phosphotransfer reaction with the phosphate immediately preceding the 3′-end, resulting in the release of the pentenal (Scheme 2).[37] The first of these reactions is analogous to that responsible for generating protein adducts with products of lipid peroxidation.[44]

In order to distinguish between the two hypotheses, we tested whether an alternative nucleophile could capture the 5′-product and thus reduce the extent of adduct formation with ALKBH1. It has been shown for β,δ-lyases, such as the Fpg protein from *E. coli*, that β-mercaptoethanol (βME) reacts with the α,β-unsaturated aldehyde produced by the β-elimination mechanism, thereby preventing the occurrence of a second elimination reaction.[45] We reasoned that, analogous to the Fpg study, this reagent may carry out a nucleophilic attack on the C3′ atom of the 5′-product and thus inhibit ALKBH1 adduct formation and lead to 5′-product release, whereas the phosphotransfer reaction would likely not be affected by its presence. Indeed, when ALKBH1 was incubated with substrate DNA containing an abasic site in the presence of βME, the free 5′-product was formed (Fig. 2A). An analysis of 3′-product release revealed that turnover rates increased from 0.0061±0.0004 min^{-1} in the absence of βME to 0.0091±0.0005 min^{-1} in the presence of the reagent (Fig. 2B). This finding supports the hypothesis that a nucleophilic residue of ALKBH1 reacts with the electrophilic C3′ of the α,β-unsaturated aldehyde of the 5′-product. To corroborate this interpretation, the sizes of native ALKBH1 and the protein-DNA adduct were determined using liquid chromatography-electrospray ionization/mass spectrometry (LC-ESI/MS). The native protein exhibited a prominent feature with m/z = 45,864 (Fig. 3A), which is in excellent agreement with the predicted size of the *C*-terminally 6xHis-tagged wild-type

(WT) protein without its *N*-terminal methionine residue. This result suggests that the large proportion of inactive enzyme is unlikely to be due to any type of covalent modification of the protein. The sample of ALKBH1 that had been incubated with a DNA substrate (oligo_AP1, Table 1) contained both WT protein and a species of m/z = 52,558 Da. This size matches the theoretically calculated mass of the protein (45,862 Da) bound to the α,β-unsaturated aldehyde of the 5′-product (6664 Da), further modified by methoxyamine (MX, 29 Da), which was used to quench the reaction (Fig. 3B). The apparent finding of substoichiometric amounts of enzyme as the protein-DNA adduct is consistent with the low level of activity for the enzyme as described above.

Time-dependence of adduct formation

Having established that the ALKBH1-DNA adduct is generated by nucleophilic attack of the enzyme on the C3′ of the α,β-unsaturated aldehyde intermediate, we examined its formation over time and compared these results to the rate of the 3′-DNA product increase. As shown in Fig. 4A–C, development of the 3′-product and formation of the ALKBH1-DNA adduct correlate, consistent with the hypothesis that generation of the two species is linked; i.e., as the DNA is cleaved to release the 3′-product, an ALKBH1 nucleophile forms a covalent bond with C3′ at the 3′-end of the 5′ product. Importantly, sodium dodecyl sulfate-polyacrylamide gel electrophoresis (SDS-PAGE) analysis revealed two distinct bands for the ALKBH1-DNA adduct, with the upper band being the more intense signal (Fig. 4B). This finding suggests that more than one species was formed, with the different protein-DNA adducts exhibiting distinct migration positions on SDS-PAGE gels while also having identical masses according to LC-ESI/MS (Fig. 3B). We postulate that more than one nucleophile can form the ALKBH1-DNA adduct; the adducts thus would retain the same total masses, but they migrate differently on SDS-PAGE gels depending on whether the nucleophile reacting with the oligonucleotide is near the middle or near a terminus of the protein.

Effects of ALKBH1 amino acid substitutions on ALKBH1-DNA adduct formation

In order to gain insights into the residues involved in forming the covalent bond with DNA, the adducts formed using different ALKBH1 variants were examined. LC-ESI/MS results provided the expected masses of the variant proteins and confirmed the presence of the expected larger sizes for variant proteins incubated with substrate DNA (data not shown). Some variants formed adducts that migrated differently during SDS-PAGE analysis when compared to the WT protein, which again exhibited an intense, slower migrating band and a less intense faster migrating species (Fig. 5A). In particular, the adducts generated with C129A, C118A/C129A (labeled D for double), and H113A/C118A/C129A/H134A (labeled Q for quadruple) variants showed much less of the slowest migrating species while forming three distinct types of protein-DNA adducts. These results highlight the importance of C129 in forming the major ALKBH1-DNA adduct, whereas the substitution of C118, K133, and H134 had little to no effect on this species. Differences in intensity of the three adduct bands between the C129A and C118A/C129A variants suggest the possible involvement of C118 in adduct formation in the C129A variant. By contrast, replacement of H113 and H134 in the quadruple variant had no further effects on ALKBH1-DNA adduct formation compared to the C118A/C129A protein. Finally, truncation of ALKBH1 by replacing the codon for

residue 347 with a stop codon (Δ347) led only to the expected smaller adduct species with no change in relative intensities of the two bands compared to WT protein. Taken together, these results suggest that C129 is responsible for forming the predominant covalent bond to the product and generating the major ALKBH1-DNA adduct. Substitution of C129 still allows for adduct formation by the reaction of other nucleophilic residues, likely to include C118, with the α,β-unsaturated aldehyde of the 5′-product.

To corroborate and extend these findings, the ALKBH1-DNA adduct was generated with selected enzyme variants and analyzed by use of a chemical protein cleavage approach. ALKBH1 samples were first incubated with 5′-FAM labeled substrate DNA then subjected to cleavage with 2-nitro-5-thiocyanobenzoic acid (NTCB), a chemical that inefficiently cleaves at the *C*-terminal side of cysteine residues.[46] The peptide-DNA adducts were analyzed by using Tris-tricine PAGE,[47] and analysis of the protein cleavage patterns focused on the three ALKBH1 peptide-DNA bands indicated on the gel (Fig. 5B and 5C). The doublet labeled C1 is absent for the sample prepared with the C304A variant and the smaller of the two bands is missing in the ALKBH1-DNA adduct generated with the C371A protein. The two signals therefore represent DNA bound to two peptides, which both start at C304 and extend to C371 or to the *C*-terminus of ALKBH1, respectively. The bands for the sample generated using the Δ347 truncation variant (labeled Δ) confirm this interpretation by revealing a single band that migrates at an apparent smaller size, in agreement with DNA bound to a fragment from C304 to A347. Band C2 is absent in C207A ALKBH1, indicating that the corresponding DNA-bound peptide either starts or ends at this residue. Since it is present in samples formed by all *C*-terminal variants examined, including the Δ347 truncation variant, this DNA-bound adduct includes the *N*-terminal region of ALKBH1. Both *N*-terminal cysteine residue variants, C118A and C129A, formed the C2 band, corroborating that this peptide-DNA adduct corresponds to a region from the *N*-terminus to C207, which is in agreement with its large size of about 25.2 kDa. It is important to emphasize that while the signal is present in the DNA-bound sample generated with the C129A protein, it is less intense. This diminished intensity is consistent with the absence of reactivity toward the α,ß-unsaturated aldehyde of the 5′ product by the primary nucleophile, while other nearby residues in this region (such as C118) can act as substitute nucleophiles to form the covalent linkage to the DNA product. In addition, the reactivity of an amino acid located in the C1 region becomes more favored in the absence of C129, as shown by the greater intensity of the C1 bands for the C129A and quadruple variants than for the WT protein. In summary, C129 is used to form the majority of the ALKBH1-DNA adduct, with other residues in this region and near the *C*-terminus forming less of the adduct; whereas in the C129A variant, a *C*-terminal residue is preferentially linked to the DNA product.

Development of a new assay to measure m^{6}A-demethylase activity of ALKBH1

Turning now to a second enzymatic activity reported for ALKBH1, the protein exhibits Fe(II)- and 2OG-dependent demethylase activity for m^{6}A in ssDNA.[34] We developed a new assay to measure this activity in which ALKBH1 was incubated with ferrous ammonium sulfate, 2OG, and an oligonucleotide containing a single m^{6}A at a DpnII restriction site. The treated oligonucleotide was annealed to its complementary strand and analyzed by a methylation-sensitive restriction digest assay (Fig. 6A). As shown in Fig. 6B, the DNA was

cleaved in an ALKBH1-dependent manner, demonstrating that the enzyme was capable of removing the lesion. Presumably, ALKBH1 hydroxylates the methyl group leading to an unstable intermediate, with loss of formaldehyde leading to restoration of the native base. Time course analysis showed that product formation increased linearly for about 30 min before the reaction decreased in rate (Fig. 6C). The activity was unexpectedly slow when compared to other demethylases; when 1 μM ALKBH1 was incubated with an equimolar amount of oligo_m6A1 for one hour at pH 7, less than 0.2 μM of the substrate was hydroxylated. No increase of activity was detected when the assay was repeated at different pH values of 6, 6.5, or 8 (data not shown). Additives such as bovine serum albumin (50 μg/ml), $MgCl_2$ (1 mM), KCl (50 mM), or NaCl (10–50 mM) did not enhance hydroxylation rates. Furthermore, removal of the 6xHis-tag of ALKBH1 did not lead to increased demethylation rates (data not shown). The activity was dependent on both the metal cofactor Fe(II) and the cosubstrate 2OG as expected for this class of enzymes. Furthermore, each of the H231A, D223A, and H287A variants, missing the three ligands for binding Fe(II), were catalytically inactive (Fig. 6D), similar to other 2OG-dependent alkylated DNA base hydroxylases like the canonical AlkB protein. In agreement with its reported specificity for ssDNA, ALKBH1 was unable to remove the methyl group when using a double-stranded (ds) substrate (Fig. 6E).

Comparison of the AP lyase and m^6A-demethylase activities for WT and variants of ALKBH1

To establish the relationship between the active sites responsible for AP lyase and m^6A-demethylase activities of ALKBH1, we directly compared these reactions in WT and variant forms of the enzyme (Fig. 7). We incubated the purified proteins with either the AP site-containing or the m^6A-containing oligonucleotide and examined the amount of product formed when using the stated conditions. For the WT protein, the measured activities were $0.012\pm0.001\ min^{-1}$ and $0.005\pm0.001\ min^{-1}$, respectively; thus, cleavage of AP-sites is about two-fold higher than removal of methyl groups on adenines. In general, the m^6A-demethylase activity was more sensitive to disruption by mutagenesis than was the AP lyase activity, with multiple variants being affected in methyl group removal and leading to more pronounced decreases in product formation. In agreement with prior reports, the K133A variant (lacking the primary residue that forms an imine with the AP substrate) and the H113A/C118A/C129A/H134A quadruple variant (affecting a putative zinc-finger domain) exhibited reduced AP lyase activity,[38, 48] consistent with other residues partially compensating to form the imine and with an important, but non-essential role for the zinc-finger domain. Whereas the K133A variant had similarly reduced levels of both activities, the quadruple variant retains ≈44% of WT enzyme activity for cleaving AP sites in DNA, but its m^6A hydroxylation capability is abolished. The H231A, D233A, and H287A Fe(II)-binding residue variants were inactive as m^6A hydroxylases, yet these variants still possess 70–75% of wild-type AP lyase activity. The C129A protein acts only at ≈10% of the WT enzyme rate on m^6A, but it retained 74% of WT enzyme activity toward AP sites. The double variant possessed 50% of WT m^6A-demethylase activity and 75% of WT AP lyase activity. In contrast to the general trend of increased susceptibility for loss of oxygenase activity, the C118A variant was as active as WT enzyme when measuring m^6A demethylase activity, but exhibited ≈80% activity as an AP lyase. These results suggest that the two

activities are at least partially independent of each other and mainly catalyzed by different residues. Of great interest, however, the predicted zinc-finger motif consisting of residues H113, C118, C129, and H134 seems to be important for both activities. This result is in agreement with the predicted flexibility of this region and its potential function in DNA recognition (SI Fig. 1).[48]

DISCUSSION

In vivo studies have identified six reactions catalyzed by ALKBH1 occurring in different cellular compartments and using distinct substrates, ranging from DNA to mRNA to tRNA to histones (Scheme 1).[30–38] Significantly, no thorough comparison of these enzymatic activities has been carried out. Here, we focused on two reactions in greater detail and performed side-by-side analyses of the AP lyase and m^6A-demethylase activities. In addition, because we had previously shown that ALKBH1 uses a β-elimination mechanism to cleave DNA at abasic sites followed by the formation of an adduct to the 5′-DNA product, we analyzed separately the AP lyase and adduct-forming reactions.[37]

We first characterized the steady-state kinetics and chemical catalysis rate of the AP lyase activity by monitoring release of the 3′-product. Steady-state kinetics revealed a turnover number of 0.028 min^{-1} that was comparable to the catalytic activities of other AP lyases. For example, histones catalyze the cleavage of AP sites in the nucleosome with k_{dis} of 0.00036 min^{-1}, while human 8-oxoguanine glycosylase (hOGG1) has a slightly higher turnover number of 0.168 min^{-1}.[43, 49] The low turnover numbers of lyases often are due to a rate-limiting step after the chemical reaction, i.e, product release slows down the overall rate.[43, 49–52] It is often speculated that slow product release is an important feature of DNA repair enzymes in order to protect the broken DNA ends from degradation. In agreement with this general behavior for lyases, time course assays revealed a biphasic curve indicating that a step after strand cleavage also is rate limiting in ALKBH1.

We subjected ALKBH1 to single-turnover assays to measure the chemical catalysis rate separately from the predicted slow product release rate after DNA cleavage. Our measured k_{obs} of 0.069 min^{-1} for ssDNA is greater than the steady-state turnover rate, confirming that DNA cleavage is faster than substrate release and not rate limiting under steady-state conditions. We also determined k_{obs} values for dsDNA with one and two AP sites and found that the rates of 0.02 min^{-1} for one AP site and 0.028 min^{-1} for two AP sites, respectively, were slower than that for ssDNA. The preference for ssDNA over dsDNA is common for AP lyases; for instance, Neil3 cleaves AP sites in ssDNA and dsDNA at rates of 0.093 min^{-1} and 0.047 min^{-1}, respectively[53]. This comparison also provide evidence that ALKBH1's chemical catalysis rate is similar to single-turnover rates of other AP lyases. Nucleosome core particles are another example; they cleave AP sites in dsDNA at 0.0014 min^{-1} [50, 51, 53] Also, while human OGG1 removes 8-oxoG rapidly from dsDNA, its AP lyase activity is only 3-fold faster than that of ALKBH1 (0.21 min^{-1}).[54]

Turning to the generation of the ALKBH1-DNA adduct, two different mechanisms were postulated for this reaction:[37] a nucleophilic residue attacking at the C3′ of the α,β-unsaturated aldehyde or catalysis of a phosphotransfer reaction with the phosphate

immediately preceding the 3′-end, resulting in the release of the pentenal (Scheme 2). In order to distinguish between these two possibilities, we used LC-ESI/MS to demonstrate that the size of the generated adduct is consistent only with the former mechanism. In other words, ALKBH1 forms a covalent bond to the α,β-unsaturated aldehyde through an attack of a nucleophilic residue at the C3′ position. The finding that MX modifies the protein-DNA adduct demonstrates the remaining presence of an aldehyde in this species. The addition of a competing nucleophile, specifically βME, reduces the extent of adduct formation in agreement with this mechanism. Taken together, these results suggest that the nucleophilic residue forming the covalent bond is positioned close to the lyase active site and able to react as soon as the product has been formed. This interpretation is also in agreement with the time course studies, which showed that protein-DNA adduct formation correlates with 3′-product formation. While DNA repair enzymes often bind tightly to their products,[50, 51, 55–57] the formation of a covalent linkage between the protein and the DNA is unusual. To the best of our knowledge, a similar scenario has only been described for PARP-1 for which a cysteine residue forms a stable crosslink with the product DNA.[55, 58]

Our detailed analysis of the properties of the ALKBH1-DNA adduct revealed another interesting feature: the formation of (at least) two distinct species. We postulate that in the WT protein, two (or more) residues are able to form a covalent bond to the 5′-DNA product of the lyase reaction. The different migration positions of the DNA-protein adduct on SDS-PAGE gels are most likely caused by their unique shapes. We identified C129 as the predominant nucleophilic residue attacking the α,β-unsaturated aldehyde, accounting for the major protein-DNA adduct. C129 is positioned in a region of the protein that is located external to the double-stranded ß-helix housing the Fe(II)- and 2OG-binding site according to the model developed by Silvestrov *et al.* (2013) (SI Figure S1).[48] Another nucleophilic residue involved in protein-DNA adduct formation is located in the *C*-terminal region, namely between C304 and C347 (excluding the cysteine residues themselves). These results confirm that at least two covalent adducts can be formed by residues in different regions of the protein. Our mass spectrometry results revealed that only a single mass species is generated for the ALKBH1-DNA adducts, so the overall sizes are identical for the different adducts. The finding that at least two residues are able to form covalent bonds with the α,β-unsaturated aldehyde is unusual, but not unprecedented. When characterizing the AP lyase activity, no single or double amino acid variant was catalytically inactive; rather, substitution of the key K133 residue only resulted in diminished activity. This phenomenon has been observed with other AP lyases and is attributed to opportunistic substitution of the primary catalytic side chain by other residues.[50, 51, 59–64] We surmise that a similar situation occurs for covalent binding of the enzyme to the product. Indeed, the two phenomena might be linked; depending on the lysine residue catalyzing the lyase reaction, different residues may form the covalent linkage. In this regard, we note that C129 is located close to the primary lysine K133; this Cys residue is therefore close to the lyase active site and may be well positioned to catalyze a nucleophilic attack at C3′ of the α,β-unsaturated aldehyde. In contrast, catalysis of the lyase reaction by a secondary lysine may result in adduct formation by an alternative residue at the *C*-terminus of the protein. This interpretation also explains the different intensities of the bands seen by SDS-PAGE for the various samples. For example, the major band using WT protein would arise via action of the primary lysine and

the primary nucleophile, while other bands are produced by secondary reactions in WT protein; these latter bands may be associated with the major reactions in samples using selected variant enzymes.

Our characterization of ALKBH1 also included a second activity, the m^6A-demethylase reaction. To more readily quantify the hydroxylation of this modified DNA base, we designed a new assay based on the incorporation of a methylation-sensitive restriction enzyme. Using this assay with ALKBH1, we demonstrated that hydroxylation of m^6A in DNA required both 2OG and Fe(II), and we showed the reaction was abolished by substituting any of the iron-binding ligands of the enzyme. This behavior has been seen for demethylation reactions of most other AlkB homologs.[7, 8, 15, 65] Unlike the rapid rates and robust behavior of mammalian Alkbh2 and Alkbh3 or bacterial AlkB,[15, 65–67] the demethylation turnover number for ALKBH1 was very low and the enzyme lost activity by 30 min, a problem that prevented extensive kinetic characterization. Our efforts to identify more favorable conditions yielding greater turnover rates for ALKBH1 were unsuccessful. Sequence specificity has not been associated with other AlkB homologs (e.g., k_{cat} values of AlkB for its preferred substrates m^1A and m^3C differ by less than two-fold using different sequences),[67] and is unlikely to be critical here. Rather, we interpret the low demethylation activity of ALKBH1 as indicating one of the following possibilities: (i) the heterologously expressed protein is less active than the native protein made in mammalian cells or (ii) we are missing an interacting protein which modulates the demethylase activity of ALKBH1 in the natural host. While Wu *et al.* (2016) showed the importance of m^6A demethylase activity in mouse ES cells,[34] this reaction may be limited to early development and not important during later stages of growth or in cell lines. Further experiments are needed to address this question.

To conclude, we characterized two of the six reported ALKBH1-dependent enzymatic activities: AP lyase and m^6A demethylase. The turnover rates were low for both reactions with the cleavage of the DNA at abasic sites being faster and more robust than the removal of the methyl group from m^6A. The demethylation reaction catalyzed by AlkB and other homologs normally proceeds quite rapidly,[15, 65–67] leading us to speculate that the ALKBH1 catalyzed hydroxylation of m^6A might not be its primary enzymatic activity in the cell. With regard to the AP lyase activity, we have previously reported that ALKBH1 has a low DNA cleavage turnover number.[37, 38] Whereas many AP lyases are limited by substrate release, a feature that can protect the cleaved DNA ends from degradation and ensure their proper re-ligation,[43, 49–52] ALKBH1 exceeds this behavior by forming a covalent bond – making this a single-turnover enzyme. A similar situation has been reported for a few other DNA cleaving enzymes. For example, the meiotic recombination enzyme Spo11 cleaves DNA according to a topoisomerase-like transphosphoesterase mechanism and binds to the 3′-product, thereby catalyzing a suicide reaction; the covalently-bound protein is released from the DNA by endonucleolytic cleavage.[68, 69] It has been hypothesized that this mechanism controls double-strand break formation during meiotic recombination in prophase I. Similarly, poly(ADP-ribose) polymerase 1 (PARP-1) forms a link to the product after incising the DNA at abasic sites. Prasad and colleagues speculated that these adducts serve as a cellular signal that indicates when base excision repair is overwhelmed or disrupted.[58] Further studies are needed to establish the importance of the m^6A-demethylase and AP lyase

activities of ALKBH1 *in vivo* and to compare these reactions to the other four enzymatic activities of this enzyme.

EXPERIMENTAL PROCEDURES

Protein production and purification

His-tagged human ALKBH1 wild-type and variant proteins were produced in *E. coli*-Codon Plus RIPL cells harboring pBAR67 and purified using a Ni-nitrilotriacetic acid Sepharose column as described previously.[37, 38] All proteins were buffer exchanged using a PD-10 disposable column (GE Healthcare Life Sciences) and stored in 20 mM Tris, pH 8, containing 1 mM EDTA (TE buffer).

AP lyase activity assays

AP lyase activity assays were carried out as described previously.[37, 38] Briefly, DNA oligonucleotides (10 μM, IDT DNA, Table 1) were incubated with uracil DNA glycosylase (2 U) to create the AP sites. For the preparation of dsDNA substrates, oligo_AP1 was annealed to either oligo_AP2 or 3, heated to 95 °C and slowly cooled to room temperature prior to the removal of the uracil and creating the AP sites. ALKBH1 was incubated with the respective substrate (1 μM) in 20 mM Tris, pH 8, containing 1 mM EDTA. For dsDNA with two AP sites, only 0.5 μM DNA was used to have equimolar amounts of AP sites in the assays. For steady-state activity assays, 0.1 – 0.4 μM protein and 1 μM substrate were incubated for 0–30 min at 37 °C in the presence of 1 mM βME. In single-turnover assays, 1 μM oligo_AP1 and 15 μM ALKBH1 were used and samples were incubated for 0–90 min at 37 °C without the addition of βME. Assays were quenched by addition of MX to a final concentration of 10 mM. In order to calculate k_{obs}, the following equation was used: Product (t) = $Substrate_{t=0}$ (1-e $^{-k(obs)*t}$).[43] Samples which were incubated with ssDNA substrates were analyzed by PAGE, whereas denaturing gels (7 M urea) were used for samples containing dsDNA. All gels were scanned with a fluorescence scanner (Typhoon FLA9500, GE Healthcare) and activities were quantified using ImageJ.[70] Rates were calculated using Graphpad Prism 6.0.

Demethylase activity assays

ALKBH1 was incubated with oligo_m6A1 (1 μM, Sigma-Aldrich, Table 1), 1 mM $Fe(NH_4)_2SO_4$, 1 mM L-ascorbic acid, and 1 mM 2OG in 50 mM bis-Tris (pH 7) at 37 °C for the indicated time periods. Reactions were stopped by heating to 95 °C after the addition of 1.1 equivalents of oligo_m6A2 and DpnII buffer. The DNA was annealed by slowly cooling the samples to room temperature at which point DpnII was added (0.5 U/μl) and the reactions were incubated at 37 °C for one hour. All samples were analyzed as described for the AP lyase activity assays.

LC-ESI/MS

In order to determine the mass of WT and variant ALKBH1, we subjected the protein samples (10 μM) to LC-ESI/MS on a Waters Acquity ultra performance liquid chromatography system coupled to a Waters Xevo G2-XS QTof mass spectrometer. The protein sample (5 μl) was injected onto a Beta-Basic CN column (10 × 1 mm, 5 μm; Thermo

Scientific) and elution was achieved by running a gradient from 98% solvent A (0.1% formic acid) to 75% solvent B (acetonitrile) at a flow rate of 0.1 ml/min. Mass spectra were obtained by electrospray ionization in positive ion mode, with a capillary voltage of 3.5 kV, a source temperature of 100 °C, desolvation temperature at 350 °C, cone gas flow at 25 l/hr and desolvation gas flow of 600 l/hr. Protein mass spectra were deconvoluted using the Advanced maximum entropy (MaxEnt) based procedure included in the Waters MassLynx software.

In order to determine the size of the protein-DNA adduct, WT and variant proteins (10 μM) were incubated with 1 μM oligo_AP1 for 3 h at 37 °C and the reaction was stopped by the addition of MX (10 mM). The samples were then subjected to LC-ESI/MS. Two distinct peaks were observed after liquid chromatography and both peaks were analyzed in order to identify potential alternative protein-DNA adducts, but none were determined.

Analysis of ALKBH1-DNA adducts by protease digestion or chemical cleavage

WT and variant forms of ALKBH1 (5 μM) were incubated with 1 μM 5′-FAM labeled substrate for 1 h at 37 °C and the reactions were stopped by addition of MX (10 mM final concentration). For chemical cleavage analysis, the samples were reduced using DTT (1 mM) in 200 mM Tris-acetate, pH 8, for 30 min at 37 °C. Cyanylation was carried out by NTCB addition and incubation for 30 min at 37 °C. The buffer was exchanged to water using a PD SpinTrap G-25 (GE Healthcare Life Sciences) and the final volume was reduced to 20 μl using Amicon 0.5 ml filters according to the manufacturer's protocols. Sodium borate (100 mM, pH 9) was added to the samples and cleavage was allowed to proceed overnight at 37 °C. All ALKBH1-DNA adduct digests and chemical cleavages were analyzed by Tris-Tricine electrophoresis[47] and the gels were scanned using a fluorescence scanner.

Supplementary Material

Refer to Web version on PubMed Central for supplementary material.

Acknowledgments

We thank Sarah L. Struble for assistance with selected experiments and Anthony Schilmiller at the MSU RTSF Mass Spectrometry and Metabolomics Core Facilities for instructions and help with the LC−ESI/MS studies.

Funding

The funding for this work was provided by the National Institutes of Health (Grant GM063582 to R.P.H.).

ABBREVIATIONS

AP	apyrimidinic/apurinic or abasic
FAM	fluorescein
LC-ESI/MS	liquid chromatography-electrospray ionization/mass spectrometry
ßME	ß-mercaptoethanol

MX	methoxyamine
NTCB	2-nitro-5-thiocyanobenzoic acid
2OG	2-oxoglutaric acid
PAGE	polyacrylamide gel electrophoresis
SDS	sodium dodecyl sulfate

References

1. Shen L, Song CX, He C, Zhang Y. Mechanism and function of oxidative reversal of DNA and RNA methylation. Annu Rev Biochem. 2014; 83:585–614. [PubMed: 24905787]
2. Wu SC, Zhang Y. Active DNA demethylation: many roads lead to Rome. Nat Rev Mol Cell Biol. 2010; 11:607–620. [PubMed: 20683471]
3. Yi C, He C. DNA repair by reversal of DNA damage. Cold Spring Harb Perspect Biol. 2013; 5:a012575. [PubMed: 23284047]
4. Schübeler D. Function and information content of DNA methylation. Nature. 2015; 517:321–326. [PubMed: 25592537]
5. Smith ZD, Meissner A. DNA methylation: roles in mammalian development. Nat Rev Genet. 2013; 14:204–220. [PubMed: 23400093]
6. Fu D, Calvo JA, Samson LD. Balancing repair and tolerance of DNA damage caused by alkylating agents. Nat Rev Cancer. 2012; 12:104–120. [PubMed: 22237395]
7. Falnes PØ, Johansen RF, Seeberg E. AlkB-mediated oxidative demethylation reverses DNA damage. Escherichia coli Nature. 2002; 419:178–182.
8. Trewick SC, Henshaw TF, Hausinger RP, Lindahl T, Sedgwick B. Oxidative demethylation by Escherichia coli AlkB directly reverts DNA base damage. Nature. 2002; 419:174–178. [PubMed: 12226667]
9. Hausinger RP. Fe(II)/α-ketoglutarate-dependent hydroxylases and related enzymes. Crit Rev Biochem Mol Biol. 2004; 39:21–68. [PubMed: 15121720]
10. Hausinger, RP. Biochemical diversity of 2-oxoglutarate-dependent oxygenases. In: Schofield, CJ., Hausinger, RP., editors. 2-Oxoglutarate-dependent oxygenases. Royal Society of Chemistry; 2015. p. 1-58.
11. Wu LF, Meng S, Tang GL. Ferrous iron and α-ketoglutarate-dependent dioxygenases in the biosynthesis of microbial natural products. Biochim Biophys Acta. 2016; 1864:453–470. [PubMed: 26845569]
12. Kurowski MA, Bhagwat AS, Papaj G, Bujnicki JM. Phylogenomic identification of five new human homologs of the DNA repair enzyme AlkB. BMC Genomics. 2003; 4:48. [PubMed: 14667252]
13. Fedeles BI, Singh V, Delaney JC, Li D, Essigmann JM. The AlkB family of Fe(II)/α-ketoglutarate-dependent dioxygenases: Repairing nucleic acid alkylation damage and beyond. J Biol Chem. 2015; 290:20734–20742. [PubMed: 26152727]
14. Müller, TA., Hausinger, RP. AlkB and its homologues – DNA repair and beyond. In: Hausinger, RP., Schofield, CJ., editors. 2-oxoglutarate dependent oxygenases. Royal Society of Chemistry; 2015. p. 246-262.
15. Aas PA, Otterlei M, Falnes PØ, Vågbø CB, Skorpen F, Akbari M, Sundheim O, Bjørås M, Slupphaug G, Seeberg E, Krokan HE. Human and bacterial oxidative demethylases repair alkylation damage in both RNA and DNA. Nature. 2003; 421:859–863. [PubMed: 12594517]
16. Duncan T, Trewick SC, Koivisto P, Bates PA, Lindahl T, Sedgwick B. Reversal of DNA alkylation damage by two human dioxygenases. Proc Natl Acad Sci USA. 2002; 99:16660–16665. [PubMed: 12486230]
17. Ringvoll J, Nordstrand LM, Vågbø CB, Talstad V, Reite K, Aas PA, Lauritzen KH, Liabakk NB, Bjørk A, Doughty RW, Falnes PØ, Krokan HE, Klungland A. Repair deficient mice reveal

mABH2 as the primary oxidative demethylase for repairing 1meA and 3meC lesions in DNA. EMBO J. 2006; 25:2189–2198. [PubMed: 16642038]

18. Li X, Xiong X, Wang K, Wang L, Shu X, Ma S, Yi C. Transcriptome-wide mapping reveals reversible and dynamic N^1-methyladenosine methylome. Nat Chem Biol. 2016; 12:311–316. [PubMed: 26863410]
19. Fu Y, Jia G, Pang X, Wang RN, Wang X, Li CJ, Smemo S, Dai Q, Bailey KA, Nobrega MA, Han KL, Cui Q, He C. FTO-mediated formation of N^6-hydroxymethyladenosine and N^6-formyladenosine in mammalian RNA. Nat Commun. 2013; 4:1798. [PubMed: 23653210]
20. Jia G, Fu Y, Zhao X, Dai Q, Zheng G, Yang Y, Yi C, Lindahl T, Pan T, Yang YG, He C. N^6-methyladenosine in nuclear RNA is a major substrate of the obesity-associated FTO. Nat Chem Biol. 2011; 7:885–887. [PubMed: 22002720]
21. Zheng G, Dahl JA, Niu Y, Fedorcsak P, Huang CM, Li CJ, Vågbø CB, Shi Y, Wang WL, Song SH, Lu Z, Bosmans RP, Dai Q, Hao YJ, Yang X, Zhao WM, Tong WM, Wang XJ, Bogdan F, Furu K, Fu Y, Jia G, Zhao X, Liu J, Krokan HE, Klungland A, Yang YG, He C. ALKBH5 is a mammalian RNA demethylase that impacts RNA metabolism and mouse fertility. Mol Cell. 2013; 49:18–29. [PubMed: 23177736]
22. Zou S, Toh JD, Wong KH, Gao YG, Hong W, Woon EC. N^6-Methyladenosine: a conformational marker that regulates the substrate specificity of human demethylases FTO and ALKBH5. Sci Rep. 2016; 6:25677. [PubMed: 27156733]
23. Dina C, Meyre D, Gallina S, Durand E, Korner A, Jacobson P, Carlsson LM, Kiess W, Vatin V, Lecoeur C, Delplanque J, Vaillant E, Pattou F, Ruiz J, Weill J, Levy-Marchal C, Horber F, Potoczna N, Hercberg S, Le Stunff C, Bougneres P, Kovacs P, Marre M, Balkau B, Cauchi S, Chevre JC, Froguel P. Variation in *FTO* contributes to childhood obesity and severe adult obesity. Nat Genet. 2007; 39:724–726. [PubMed: 17496892]
24. Frayling TM, Timpson NJ, Weedon MN, Zeggini E, Freathy RM, Lindgren CM, Perry JR, Elliott KS, Lango H, Rayner NW, Shields B, Harries LW, Barrett JC, Ellard S, Groves CJ, Knight B, Patch AM, Ness AR, Ebrahim S, Lawlor DA, Ring SM, Ben-Shlomo Y, Jarvelin MR, Sovio U, Bennett AJ, Melzer D, Ferrucci L, Loos RJ, Barroso I, Wareham NJ, Karpe F, Owen KR, Cardon LR, Walker M, Hitman GA, Palmer CN, Doney AS, Morris AD, Smith GD, Hattersley AT, McCarthy MI. A common variant in the *FTO* gene is associated with body mass index and predisposes to childhood and adult obesity. Science. 2007; 316:889–894. [PubMed: 17434869]
25. van den Born E, Vågbø CB, Songe-Møller L, Leihne V, Lien GF, Leszczynska G, Malkiewicz A, Krokan HE, Kirpekar F, Klungland A, Falnes PØ. ALKBH8-mediated formation of a novel diastereomeric pair of wobble nucleosides in mammalian tRNA. Nat Commun. 2011; 2:172. [PubMed: 21285950]
26. Li MM, Nilsen A, Shi Y, Fusser M, Ding YH, Fu Y, Liu B, Niu Y, Wu YS, Huang CM, Olofsson M, Jin KX, Lv Y, Xu XZ, He C, Dong MQ, Rendtlew Danielsen JM, Klungland A, Yang YG. ALKBH4-dependent demethylation of actin regulates actomyosin dynamics. Nat Commun. 2013; 4:1832. [PubMed: 23673617]
27. Fu D, Jordan JJ, Samson LD. Human ALKBH7 is required for alkylation and oxidation-induced programmed necrosis. Genes Dev. 2013; 27:1089–1100. [PubMed: 23666923]
28. Solberg A, Robertson AB, Aronsen JM, Rognmo Ø, Sjaastad I, Wisløff U, Klungland A. Deletion of mouse *Alkbh7* leads to obesity. J Mol Cell Biol. 2013; 5:194–203. [PubMed: 23572141]
29. Pan Z, Sikandar S, Witherspoon M, Dizon D, Nguyen T, Benirschke K, Wiley C, Vrana P, Lipkin SM. Impaired placental trophoblast lineage differentiation in $Alkbh1^{-/-}$ mice. Dev Dyn. 2008; 237:316–327. [PubMed: 18163532]
30. Müller TA, Yu K, Hausinger RP, Meek K. ALKBH1 is dispensable for abasic site cleavage during base excision repair and class switch recombination. PLoS One. 2013; 8:e67403. [PubMed: 23825659]
31. Nordstrand LM, Svärd J, Larsen E, Nilsen A, Ougland R, Furu K, Lien GF, Rognes T, Namekawa SH, Lee JT, Klungland A. Mice lacking Alkbh1 display sex-ratio distortion and unilateral eye defects. PLoS One. 2010; 5:e13827. [PubMed: 21072209]
32. Westbye MP, Feyzi E, Aas PA, Vågbø CB, Talstad VA, Kavli B, Hagen L, Sundheim O, Akbari M, Liabakk NB, Slupphaug G, Otterlei M, Krokan HE. Human AlkB homolog 1 is a mitochondrial

protein that demethylates 3-methylcytosine in DNA and RNA. J Biol Chem. 2008; 283:25046–25056. [PubMed: 18603530]

33. Ougland R, Lando D, Jonson I, Dahl JA, Moen MN, Nordstrand LM, Rognes T, Lee JT, Klungland A, Kouzarides T, Larsen E. ALKBH1 is a histone H2A dioxygenase involved in neural differentiation. Stem Cells. 2012; 30:2672–2682. [PubMed: 22961808]
34. Wu TP, Wang T, Seetin MG, Lai Y, Zhu S, Lin K, Liu Y, Byrum SD, Mackintosh SG, Zhong M, Tackett A, Wang G, Hon LS, Fang G, Swenberg JA, Xiao AZ. DNA methylation on N^6-adenine in mammalian embryonic stem cells. Nature. 2016; 532:329–333. [PubMed: 27027282]
35. Haag S, Sloan KE, Ranjan N, Warda AS, Kretschmer J, Blessing C, Hubner B, Seikowski J, Dennerlein S, Rehling P, Rodnina MV, Hobartner C, Bohnsack MT. NSUN3 and ABH1 modify the wobble position of mt-$tRNA^{Met}$ to expand codon recognition in mitochondrial translation. EMBO J. 2016; 35:2104–2119. [PubMed: 27497299]
36. Liu F, Clark W, Luo G, Wang X, Fu Y, Wei J, Wang X, Hao Z, Dai Q, Zheng G, Ma H, Han D, Evans M, Klungland A, Pan T, He C. ALKBH1-mediated tRNA demethylation regulates translation. Cell. 2016; 167:816–828. [PubMed: 27745969]
37. Müller TA, Andrzejak MM, Hausinger RP. A covalent protein-DNA 5′-product adduct is generated following AP lyase activity of human ALKBH1 (AlkB homologue 1). Biochem J. 2013; 452:509–518. [PubMed: 23577621]
38. Müller TA, Meek K, Hausinger RP. Human AlkB homologue 1 (ABH1) exhibits DNA lyase activity at abasic sites. DNA Repair (Amst). 2010; 9:58–65. [PubMed: 19959401]
39. Korvald H, Falnes PØ, Laerdahl JK, Bjørås M, Alseth I. The *Schizosaccharomyces pombe* AlkB homolog Abh1 exhibits AP lyase activity but no demethylase activity. DNA Repair (Amst). 2012; 11:453–462. [PubMed: 22365419]
40. Larijani M, Petrov AP, Kolenchenko O, Berru M, Krylov SN, Martin A. AID associates with single-stranded DNA with high affinity and a long complex half-life in a sequence-independent manner. Mol Cell Biol. 2007; 27:20–30. [PubMed: 17060445]
41. Yu K, Lieber MR. The nicking step in V(D)J recombination is independent of synapsis: implications for the immune repertoire. Mol Cell Biol. 2000; 20:7914–7921. [PubMed: 11027262]
42. Porello SL, Leyes AE, David SS. Single-turnover and pre-steady-state kinetics of the reaction of the adenine glycosylase MutY with mismatch-containing DNA substrates. Biochemistry. 1998; 37:14756–14764. [PubMed: 9778350]
43. Sassa A, Beard WA, Shock DD, Wilson SH. Steady-state, pre-steady-state, and single-turnover kinetic measurement for DNA glycosylase activity. J Vis Exp. 2013:e50695. [PubMed: 23995844]
44. Sayre LM, Lin D, Yuan Q, Zhu X, Tang X. Protein adducts generated from products of lipid oxidation: focus on HNE and one. Drug Metab Rev. 2006; 38:651–675. [PubMed: 17145694]
45. Bhagwat M, Gerlt JA. 3′- and 5′-strand cleavage reactions catalyzed by the Fpg protein from *Escherichia coli* occur via successive β- and δ-elimination mechanisms, respectively. Biochemistry. 1996; 35:659–665. [PubMed: 8555240]
46. Crimmins, DL., Mische, SM., Denslow, ND. Curr Protoc Protein Sci. John Wiley & Sons, Inc; 2005. Chemical cleavage of proteins in solution. Unit 11.14.11 - 11.14.11
47. Schägger H. Tricine-SDS-PAGE. Nat Protoc. 2006; 1:16–22. [PubMed: 17406207]
48. Silvestrov P, Müller TA, Clark KN, Hausinger RP, Cisneros GA. Homology modeling, molecular dynamics, and site-directed mutagenesis study of AlkB human homolog 1 (ALKBH1). J Mol Graph Model. 2014; 54:123–130. [PubMed: 25459764]
49. Zhou C, Greenberg MM. Histone-catalyzed cleavage of nucleosomal DNA containing 2-deoxyribonolactone. J Am Chem Soc. 2012; 134:8090–8093. [PubMed: 22551239]
50. Sczepanski JT, Wong RS, McKnight JN, Bowman GD, Greenberg MM. Rapid DNA-protein cross-linking and strand scission by an abasic site in a nucleosome core particle. Proc Natl Acad Sci USA. 2010; 107:22475–22480. [PubMed: 21149689]
51. Sczepanski JT, Zhou C, Greenberg MM. Nucleosome core particle-catalyzed strand scission at abasic sites. Biochemistry. 2013; 52:2157–2164. [PubMed: 23480734]
52. Vik ES, Alseth I, Forsbring M, Helle IH, Morland I, Luna L, Bjoras M, Dalhus B. Biochemical mapping of human NEIL1 DNA glycosylase and AP lyase activities. DNA Repair (Amst). 2012; 11:766–773. [PubMed: 22858590]

53. Liu M, Bandaru V, Bond JP, Jaruga P, Zhao X, Christov PP, Burrows CJ, Rizzo CJ, Dizdaroglu M, Wallace SS. The mouse ortholog of NEIL3 is a functional DNA glycosylase in vitro and in vivo. Proc Natl Acad Sci USA. 2010; 107:4925–4930. [PubMed: 20185759]
54. Dalhus B, Forsbring M, Helle IH, Vik ES, Forstrom RJ, Backe PH, Alseth I, Bjoras M. Separation-of-function mutants unravel the dual-reaction mode of human 8-oxoguanine DNA glycosylase. Structure. 2011; 19:117–127. [PubMed: 21220122]
55. Khodyreva SN, Prasad R, Ilina ES, Sukhanova MV, Kutuzov MM, Liu Y, Hou EW, Wilson SH, Lavrik OI. Apurinic/apyrimidinic (AP) site recognition by the 5′-dRP/AP lyase in poly(ADP-ribose) polymerase-1 (PARP-1). Proc Natl Acad Sci USA. 2010; 107:22090–22095. [PubMed: 21127267]
56. Kuznetsov NA, Zharkov DO, Koval VV, Buckle M, Fedorova OS. Reversible chemical step and rate-limiting enzyme regeneration in the reaction catalyzed by formamidopyrimidine-DNA glycosylase. Biochemistry. 2009; 48:11335–11343. [PubMed: 19835417]
57. Pinz KG, Bogenhagen DF. Characterization of a catalytically slow AP lyase activity in DNA polymerase γ and other family A DNA polymerases. J Biol Chem. 2000; 275:12509–12514. [PubMed: 10777538]
58. Prasad R, Horton JK, Chastain PD 2nd, Gassman NR, Freudenthal BD, Hou EW, Wilson SH. Suicidal cross-linking of PARP-1 to AP site intermediates in cells undergoing base excision repair. Nucleic Acids Res. 2014; 42:6337–6351. [PubMed: 24771347]
59. Strande N, Roberts SA, Oh S, Hendrickson EA, Ramsden DA. Specificity of the dRP/AP lyase of Ku promotes nonhomologous end joining (NHEJ) fidelity at damaged ends. J Biol Chem. 2012; 287:13686–13693. [PubMed: 22362780]
60. Postel EH. Cleavage of DNA by human NM23-H2/nucleoside diphosphate kinase involves formation of a covalent protein-DNA complex. J Biol Chem. 1999; 274:22821–22829. [PubMed: 10428867]
61. Postel EH, Abramczyk BM, Levit MN, Kyin S. Catalysis of DNA cleavage and nucleoside triphosphate synthesis by NM23-H2/NDP kinase share an active site that implies a DNA repair function. Proc Natl Acad Sci USA. 2000; 97:14194–14199. [PubMed: 11121025]
62. Prasad R, Beard WA, Chyan JY, Maciejewski MW, Mullen GP, Wilson SH. Functional analysis of the amino-terminal 8-kDa domain of DNA polymerase β as revealed by site-directed mutagenesis. DNA binding and 5′-deoxyribose phosphate lyase activities. J Biol Chem. 1998; 273:11121–11126. [PubMed: 9556598]
63. Rajan R, Prasad R, Taneja B, Wilson SH, Mondragón A. Identification of one of the apurinic/apyrimidinic lyase active sites of topoisomerase V by structural and functional studies. Nucleic Acids Res. 2013; 41:657–666. [PubMed: 23125368]
64. Rajan R, Osterman A, Mondragon A. *Methanopyrus kandleri* topoisomerase V contains three distinct AP lyase active sites in addition to the topoisomerase active site. Nucleic Acids Res. 2016; 44:3464–3474. [PubMed: 26908655]
65. Lee DH, Jin SG, Cai S, Chen Y, Pfeifer GP, O'Connor TR. Repair of methylation damage in DNA and RNA by mammalian AlkB homologues. J Biol Chem. 2005; 280:39448–39459. [PubMed: 16174769]
66. Koivisto P, Duncan T, Lindahl T, Sedgwick B. Minimal methylated substrate and extended substrate range of *Escherichia coli* AlkB protein, a 1-methyladenine-DNA dioxygenase. J Biol Chem. 2003; 278:44348–44354. [PubMed: 12944387]
67. Yu B, Hunt JF. Enzymological and structural studies of the mechanism of promiscuous substrate recognition by the oxidative DNA repair enzyme AlkB. Proc Natl Acad Sci USA. 2009; 106:14315–14320. [PubMed: 19706517]
68. Keeney S, Giroux CN, Kleckner N. Meiosis-specific DNA double-strand breaks are catalyzed by Spo11, a member of a widely conserved protein family. Cell. 1997; 88:375–384. [PubMed: 9039264]
69. Keeney S, Lange J, Mohibullah N. Self-organization of meiotic recombination initiation: general principles and molecular pathways. Annu Rev Genet. 2014; 48:187–214. [PubMed: 25421598]
70. Rasband, WS. ImageJ. Health, U.S.I.o.. , editor. US National Institutes of Health; Bethesda: 1997–2016.

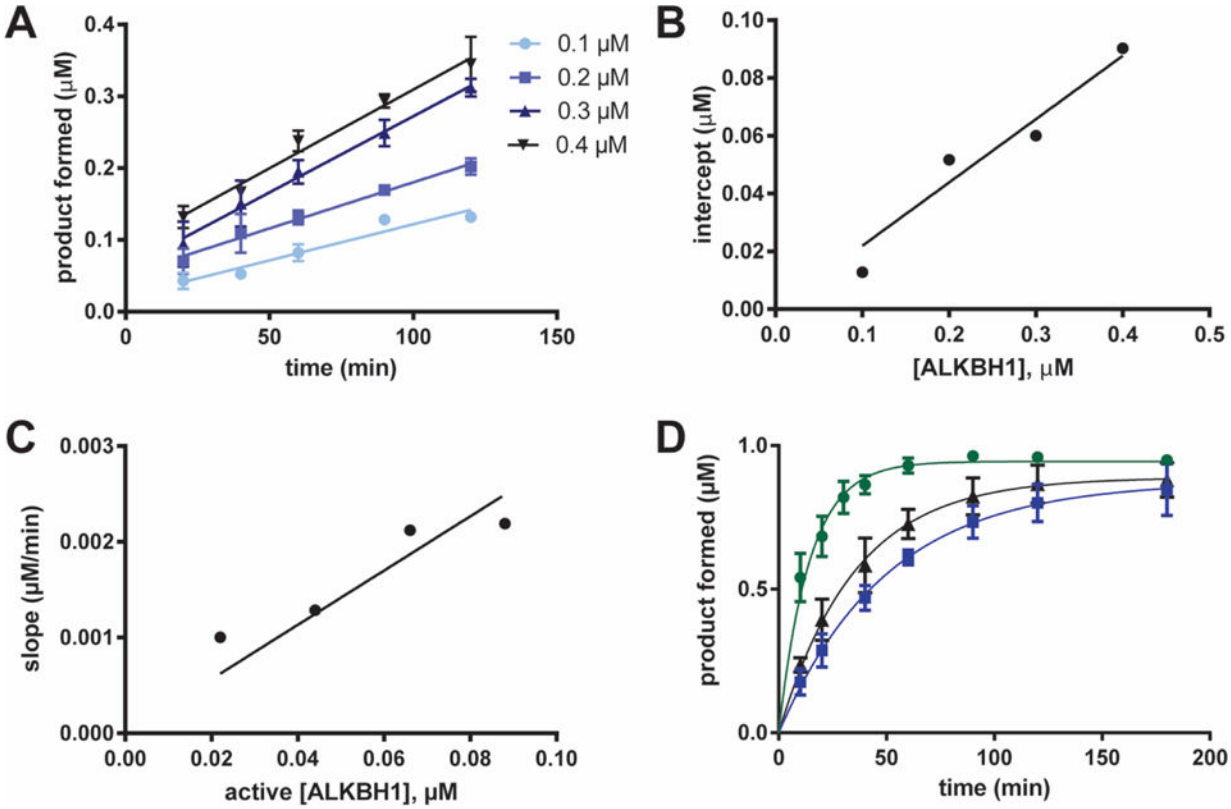

Figure 1.

Kinetic characterization of AP lyase activity of ALKBH1 on the basis of 3′-product release. (A) Determination of turnover rates under steady-state conditions. ALKBH1 was incubated at the indicated concentrations with 1 μM 3′-FAM-labeled oligo_AP1 in the presence of 1 mM βME at pH 8 and 37 °C, and product formation was measured at the different time points. We analyzed three to five independent experiments by ImageJ with the averages calculated and plotted. (B) Determination of active protein fraction. The ALKBH1 concentrations used in the assays were plotted against the intercepts of the lines shown in panel A. The resulting slope of 22.0±1.4% represents the active protein concentration. (C) Determination of steady-state turnover rate. We plotted the active ALKBH1 concentrations in the assays against the slopes of the lines shown in panel A. The resulting slope represents the turnover rate of 0.028±0.003 min^{-1}. (D) Determination of product formation under single-turnover conditions. ALKBH1 (15 μM) was incubated with one μM of either ssDNA substrate (oligo_AP1, shown in green) or dsDNA containing one AP site (oligo_AP1 annealed to oligoAP_2, in blue) or two AP sites (oligoAP_1 annealed to oligo_AP3, in black) at pH 8 and 37 °C for the times indicated. The data were fit as described in the Experimental Procedures to estimate the k_{obs} associated with the chemical step for DNA cleavage by ALKBH1.

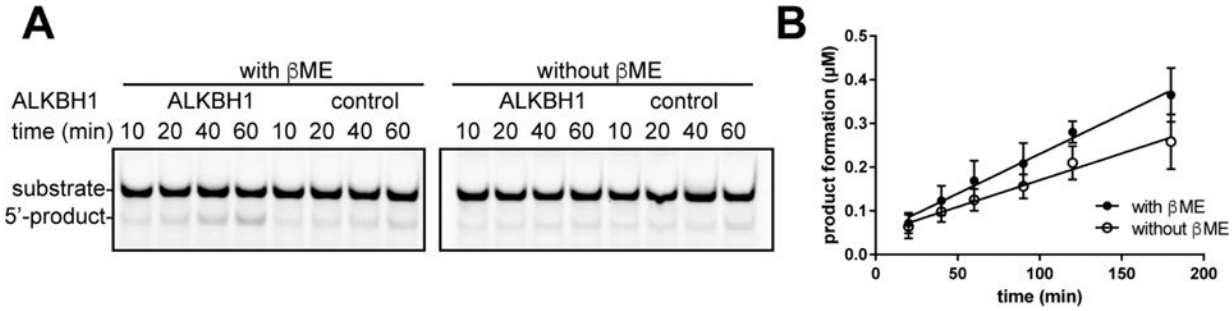

Figure 2.

The 5′-product released by ALKBH1's AP lyase activity increases in the presence of βME. (A) Representative PAGE gels showing 5′-product formation in the presence or absence of βME. ALKBH1 (0.2 μM) was incubated with 5′-FAM-labeled oligo_AP1 (1 μM) with or without βME (1 mM) for the indicated time points and analyzed by PAGE. The control samples lacked enzyme to monitor unspecific cleavage. (B) Analysis of 3′-product formation over time in the presence and absence of βME. Three to five independent experiments were analyzed by ImageJ, the amount of product formed relative to the amount of enzyme was calculated for each timepoint, and the average percentages were plotted. The rates of product formation are 0.0091±0.0005 min^{-1} with βME and 0.0061±0.0004 min^{-1} without βME.

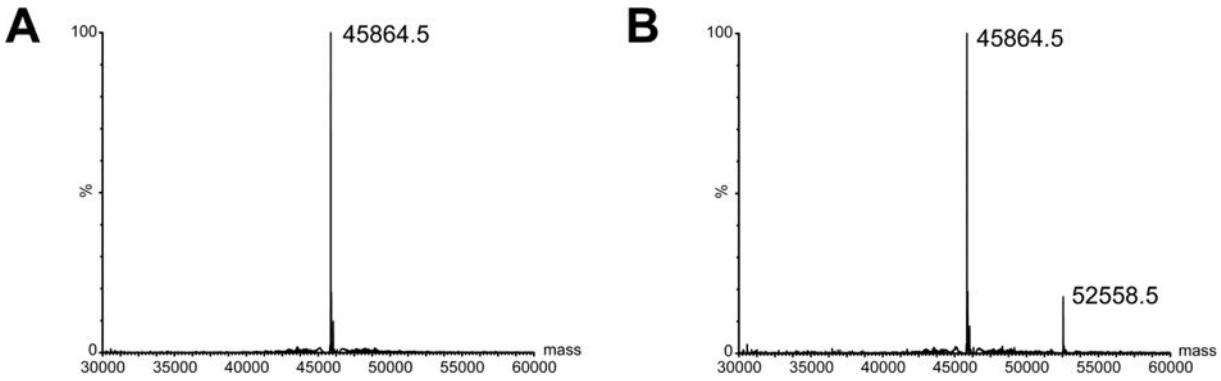

Figure 3.

Determination of the size of native ALKBH1 and its protein-DNA adduct using LC-ESI/MS. (A) LC-ESI/MS analysis of native ALKBH1 (10 μM). (B) LC-ESI/MS analysis of the ALKBH1-DNA adduct. ALKBH1 (10 μM) was incubated with 1 μM oligo_AP1 for 3 h, the reaction was stopped by addition of 0.1 M MX and the sample was subjected to LC-ESI/MS.

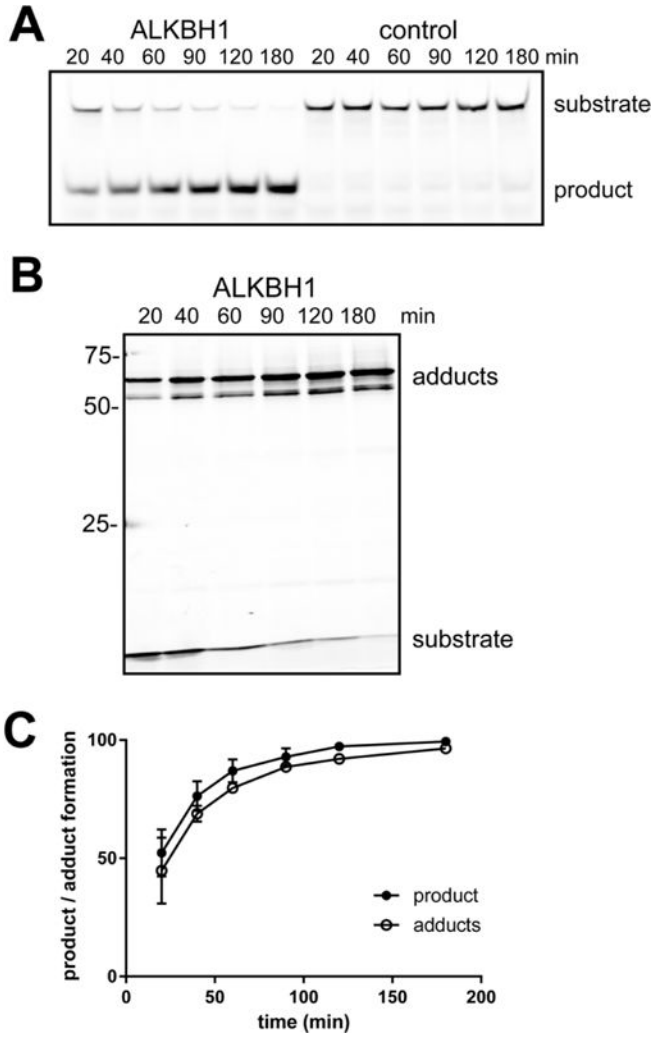

Figure 4.

Kinetics of adduct formation of ALKBH1 with its 5′-product and comparison to release of the 3′-product. (A) Representative PAGE gel showing 3′-product formation over time. ALKBH1 (5 μM) was incubated with 3′-FAM-labeled oligo_AP1 (1 μM) at 37 °C and product formation was analyzed at the indicated time points by PAGE. The control sample lacks protein and monitors unspecific cleavage of the AP site. (B) Representative SDS-PAGE gel illustrating adduct formation of ALKBH1 with 5′-product over time. ALKBH1 was incubated with 5′-FAM-labeled oligo_AP1 as described in panel A and adduct formation was analyzed by SDS-PAGE. (C) Adduct and product formation over time. Gels from three to five independent experiments were analyzed by ImageJ, and averages were calculated and plotted. Assays were carried out in the absence of βME.

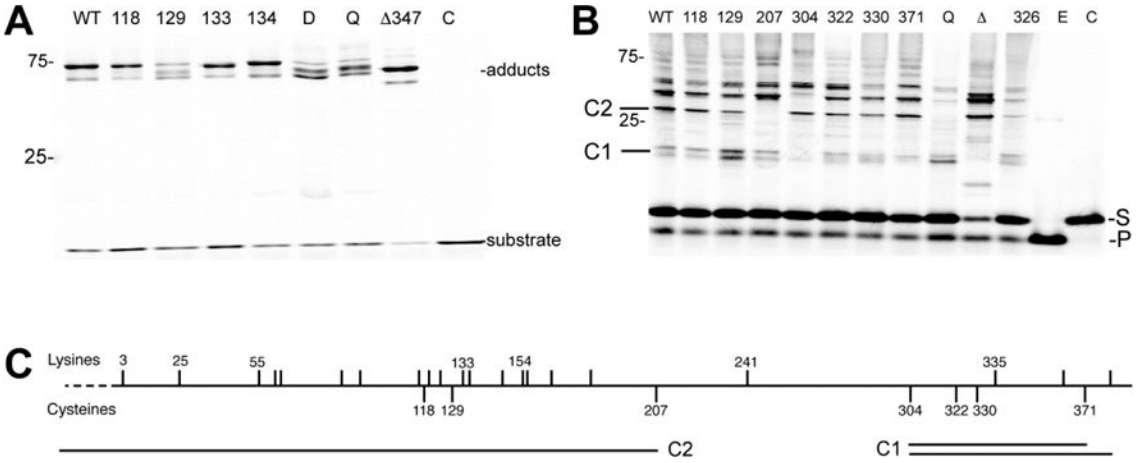

Figure 5.

Adduct formation of ALKBH1 and selected variants with the 5′-DNA product. (A) ALKBH1 WT and variants (5 μM) were incubated with 5′-FAM labeled oligo_AP1 for 1 h at 37 °C, the reaction was stopped by addition of MX, and adduct formation was analyzed by SDS-PAGE. (B) NTCB cleavage of the protein-DNA adduct for WT and variant forms of ALKBH1. ALKBH1 and its variants were incubated with DNA as described in panel A and then subjected to chemical cleavage at Cys residues by NTCB as described in the Experimental Procedures. E stands for endonuclease III, another AP lyase, which was incubated with the substrate DNA in order to cleave the oligonucleotide at the abasic site and visualize the size of the product on the gel. The samples were analyzed by Tris-tricine SDS-PAGE. For all gel analysis, FAM-labeled DNA was detected using a fluorescence scanner. (C) Scheme depicting ALKBH1 with the positions indicated for its 22 Lys and 7 Cys residues. Underneath are the corresponding protein fragments for the adducts seen on the Tris-tricine gel of panel B.

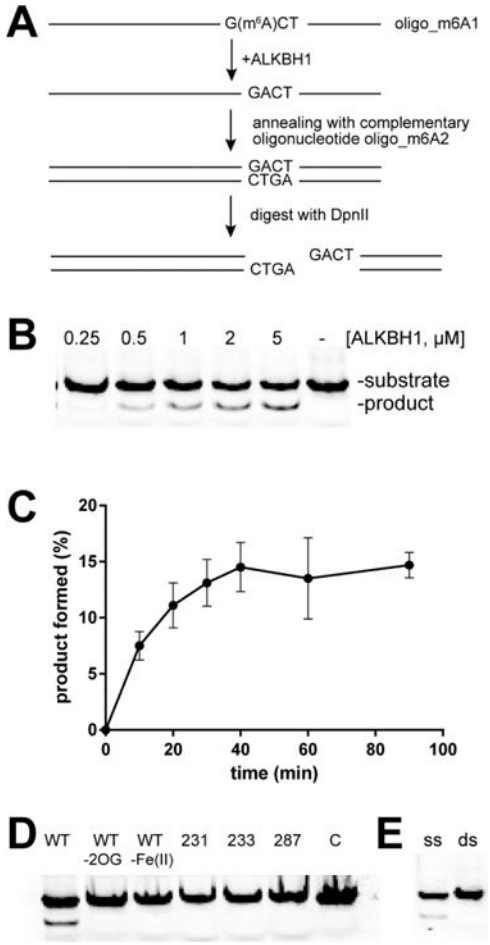

Figure 6.

m^6A Demethylation activity of ALKBH1. (A) Scheme of the assay. A m^6A-containing oligonucleotide is incubated with ALKBH1 in the presence of Fe(II) and 2OG. After the assay, ALKBH1 is inactivated by heating to 95 °C and the ssDNA substrate is annealed to the complementary oligonucleotide by slowly cooling to room temperature. The reaction is then digested with DpnII, a methylation-sensitive restriction enzyme that cleaves the ds oligonucleotide only if the methyl group on the adenine has been removed. (B) Representative PAGE gel reporting the m^6A-demethylase activity of ALKBH1. Different concentrations of ALKBH1 were incubated with oligo_m6A1 (1 μM), Fe(II) (1 mM), and 2OG (2 mM) for 1 h, then treated according to the scheme shown in panel A and analyzed by PAGE. (C) Time course of the reaction. ALKBH1 (1 μM) was incubated with 1 μM oligo_m6A1, cofactor, and cosubstrate, and the reaction was stopped at the indicated time points. Three independent experiments were used to calculate the average demethylation activity and the error bars represent the standard deviation. (D) The m^6A-demethylase activity of ALKBH1 requires Fe(II) and 2OG, and is abolished in the iron-ligand variants H231A, D233A, and H287A. WT ALKBH1 (1 μM) was incubated with or without Fe(II) (1 mM) and 2OG (2 mM) and oligo_m6A1 (1 M) for 1 h at 37 °C and analyzed as before. The variants were analyzed similarly. (E) ALKBH1 demethylates ssDNA containing m^6A, but not hemimethylated DNA. ALKBH1 (1 μM) was incubated with either ss oligo_m6A1 or

oligo_m6A1 annealed to oligo_m6A2 containing one m^6A site (1 μM) for 1 h and then treated and analyzed as described in panel B.

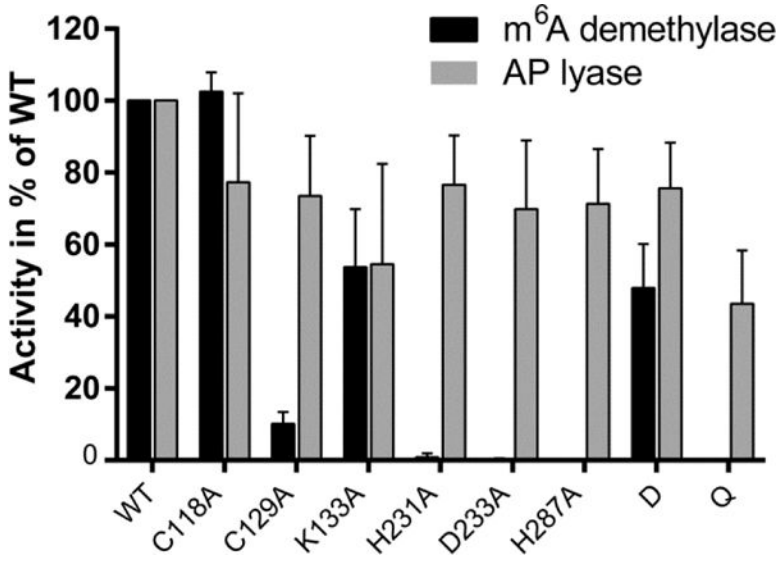

Figure 7.

Comparison of m^6A-demethylase and AP lyase activities of WT and variant forms of ALKBH1. ALKBH1 and selected variants (1 μM) were incubated with either oligo_m6A1 or oligo_AP1 (1 μM) for 30 min at 37 °C, then analyzed as described in Experimental Procedures. Three to five independent assays were used to calculate averages and standard deviations. The activities of the WT protein (0.005±0.001 min^{-1} for m^6A demethylation and 0.012±0.001 min^{-1} for AP lyase) were set to 100% for comparison the activities of the variant proteins.

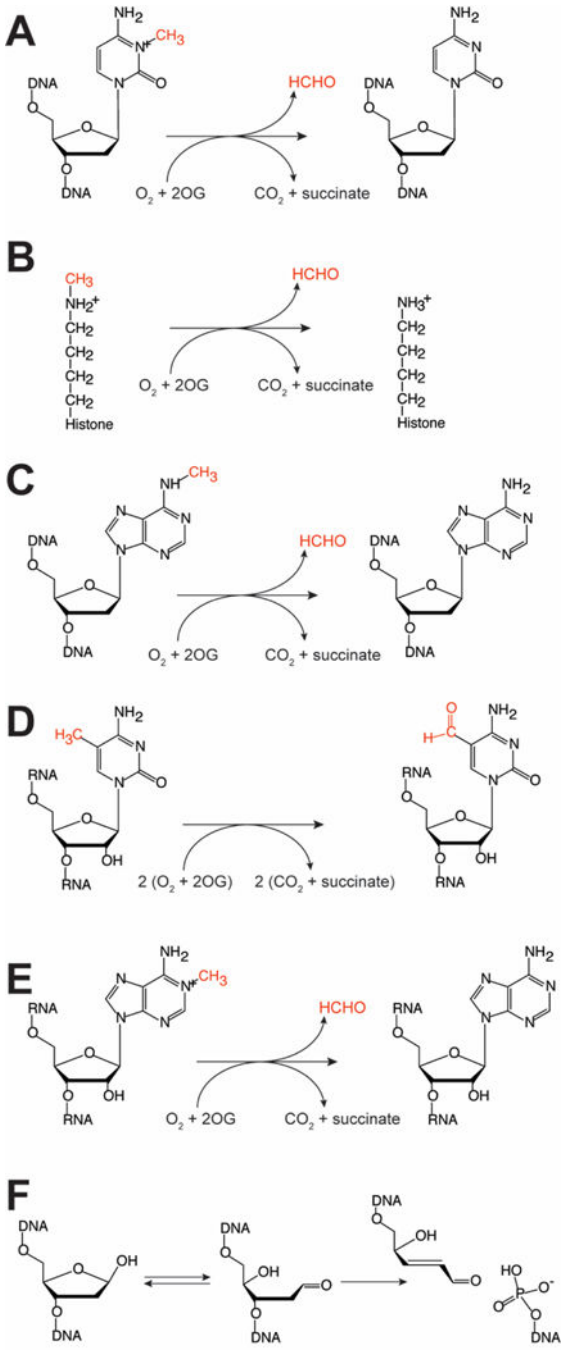

Scheme 1.

Enzymatic activities reported for mammalian Alkbh1 *in vitro*[a]

[a]Key: (A) Demethylation of m^3C in DNA.[32] (B) Demethylation of methylated lysine in histone H2A (demonstrated only in a cell-based assay).[33] (C) Demethylation of m^6A in DNA.[34] (D) Double hydroxylation of m^5C in mitochondrial tRNA.[35] (E) Demethylation of m^1A in tRNA.[36] (F) Lyase cleavage of AP sites in DNA (this reaction is independent of Fe(II) and 2OG).[38]

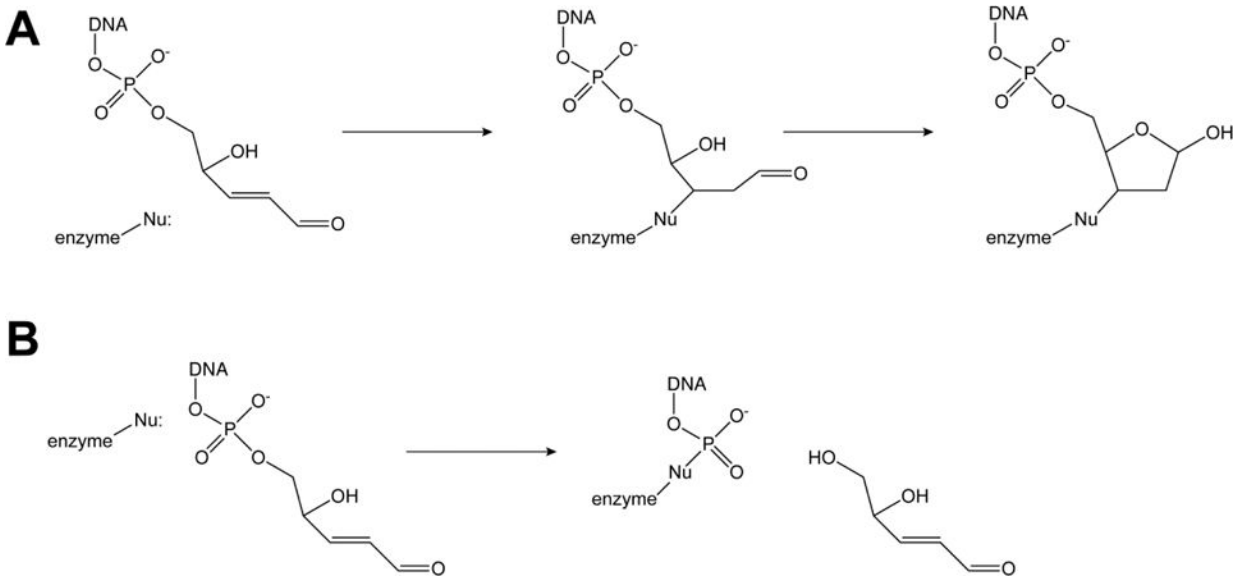

Scheme 2.

Table 1

Oligonucleotides used in this study

Name	Sequence	comment
oligo_AP1	5′-AACTTCGTGCAGGCATGGTAG(dU)TTGTCTACT-3′	31-mer containing dU, 5′- or 3′-FAM labeled
Oligo_AP2	5-AGTAGACAAGCTACCATGCCTGCACGAAGTT-3	31-mer, reverse complement of oligo_AP1 with dC instead of dU
Oligo_AP3	5′-AGTAGACA $AG(dU)\mathrm{T}_{\mathrm{ACCATGCCTGCACGA}}\,AGTT$-3′	31-mer containing dU, reverse complement of oligo_AP1 with dG opposite dU
oligo_m6A1	5′-AACTTCGTGCAGGCATGGG(m^{6}A)TCTTGTCTACT-3′	31-mer containing m^{6}A in DpnII restriction site (underlined); 5′-FAM labeled
oligo_m6A2	5′-AGTAGACAAGATCCCATGCCTGCACGAAGTT-3′	31-mer, reverse complement of oligo_m6A-1 with DpnII restriction site (underlined)